DOI:10.1190/4D-Forum2024-015.1

Time-lapse model by 4D dynamic matching joint full waveform inversion

Fuchun Gao, David Cavalin, Daniel Davies, Faqi Liu, Lee Saxton, Carlos Calderon, TGS
Philip Tillotson, Lifeng Wang, BP

Summary

The 4D seismic method has been increasingly applied since being introduced some four decades ago for reservoir monitoring including pressure changes and fluid replacements. At the same time, seismic imaging technique has been steadily improved in term of resolution, driven by advances in data acquisition and imaging algorithms. Most notably, full waveform inversion (FWI) has been widely applied due to its resolving power for sub-surface structures. However, it is still a challenge to reliably obtain a 4DFWI model that is genuinely attributed to changes in reservoir since other factors such as non-repeatability of data acquisition between baseline and monitor surveys can contribute to time-lapse data differences as well. In this study, we propose and implement a 4D joint inversion scheme formulated in the framework of dynamic matching FWI (DM FWI) and applied it to obtain a high resolution 4D model using datasets acquired in the North Sea over an active reservoir zone. The 4D joint inversion offers efficient turn-around while producing coherent 4D velocity model responses.

Introduction

With the advancements in imaging techniques and improved repeatability in data acquisition, time-lapse (4D) seismic processing and imaging provide valuable information about the subsurface. Conventionally most 4D processing approaches rely on imaging workflows that process baseline and monitor datasets using a similar, if not identical, processing sequence. These methods infer time-lapse changes in fluid saturation and pressure by qualitatively and/or quantitatively interpreting differences in the resulting migration images (e.g., Anderson et al., 2005; Lumley, 2001; Meek et al., 2017). In addition to 4D changes through interpretation on migrated images, changes of physical reservoir properties can be retrieved directly through inversion, taking advantage of the resolving power of FWI which has been widely applied to conventional 3D seismic data to obtain high resolution velocity models (e.g., Sirgue et al., 2011; Routh et al., 2023). More recently, a number of 4DFWI algorithms with different variations have been proposed and implemented to directly invert time-lapse model differences in marine settings for reservoir monitoring (e.g., Yang et al., 2013; Musa et al., 2015; Liu and Tsvankin, 2022; Dutta et al., 2023; Pintus et al., 2023). One of the challenges that 4DFWI faces is the non-repeatability of data acquisitions (Zhou and Lumley, 2020). Even if the acquisition geometry of both baseline and monitor surveys are close enough (source and receiver positioning), other survey variations such as different sea levels, water temperatures and noise levels might introduce false 4D anomalies into the time-lapse model if not properly addressed. To overcome differences in noise level, a noise-resilient 4DFWI algorithm is needed, as noise issues may persist after the 4D pre-processing in time-domain. Spatial misalignments between two data acquisition geometries widely exist, and it can be typically resolved through data regularization. However, it is impossible to align two datasets with good accuracy in cases such as two narrow azimuth acquisitions with strong feathering. In the case where the 4D signature in time domain is weak and small in magnitude, it is not ideal to align the base and monitor datasets as errors introduced during regularization could be at the same level as the target 4D signature. Additionally, it can be time-consuming to align two datasets using a high-dimensional regularization method. For these reasons, we require a 4DFWI algorithm that is noise-resilient, reliable and insensitive to misalignments between acquisition geometries. In this study, we propose and implement such an algorithm based on 4D joint inversion in the framework of DM FWI (Mao et al., 2020). We show its application to 4D OBN datasets acquired in the North Sea in 2017 and 2023 over an active production field. DM FWI has been widely applied to 3D datasets in both marine and land settings, achieving high resolution FWI velocity models and FWI images, the pseudo-reflectivity derived from FWI models (Yong et al., 2023; Romanenko et al., 2023). It has proven to be noise-resilient and robust that, together with a specially designed workflow, the acoustic DM FWI can be successfully applied to data with severe elastic effects (Gao et al., 2023).

This paper is organized as follows. We introduce the 4DFWI algorithm and the motivation behind it, followed by its application to 4D OBN datasets. Finally, we discuss the technical aspects involved in the application, and draw observations and conclusions.

Method

This section introduces the theoretical background of DM FWI and then elaborates on the 4DFWI by joint inversion. DM FWI updates the model by maximizing the similarity between the observed data *d(t)* and the synthetic data *u(t)* that is measured by the following objective function:

$$E(m) = \sum_{s,r,j} c(s,r,j) \quad (1)$$

where *c(s,r,j)* is the local cross-correlation of an observed data *d(t)* and a dynamically matched version of the synthetic

DOI:10.1190/4D-Forum2024-015.1

data *u(t)* simulated using model *m*, through local amplitude normalization, thus making the data matching less sensitive to amplitude discrepancies due to noises.

The proposed 4DFWI algorithm that jointly inverts baseline and monitor datasets intends to minimize the following objective function:

$$E(m_{base}, m_{monitor}) = \sum_{s,r,j}\left[\frac{1}{2} - \frac{1}{2}c_{base}(s,r,j)\right] + \sum_{s,r,j}\left[\frac{1}{2} - \frac{1}{2}c_{monitor}(s,r,j)\right] + \alpha\left|\left|R(m_{monitor} - m_{base})\right|\right|^{p} \quad (2)$$

where R is a regularization function which could be a mask function, α is the damping coefficient which defines the relative weight of the third term on the right hand of Equation (2), and p is either 1 or 2, the norm of the 4D model. Minimizing the first and second term on the right-hand side of Equation (2) is equivalent to maximizing the 3D DM FWI objective function defined in Equation (1) using either dataset respectively. The third term applies a 4D model regularization, penalizing the difference between the two models being jointly updated. The final baseline and monitor models are then the models with minimum difference between them (measured in the L1 or L2 norms), yet each predicts its respective observed data well. One of the advantages of 4D joint inversion is that the two datasets do not have to be perfectly aligned, although it is assumed that the two acquisition geometries are near each other spatially.

For gradient-based FWI, the algorithm is realized by alternating updates between the baseline and monitor models by deriving gradient with respect to either of them at one iteration. After one model is updated for *n* iterations where $n \in [1,3]$ in our practice, it will be used and fixed inside the 3rd term on the right hand of Equation (2) for the next alternation of update on the other model, and so on so forth until the iterations finish based on certain criteria.

Application to the OBN datasets

The 4D datasets in this study are from dense OBN surveys in the North Sea (Tillotson et al., 2019) over the Clair field, with baseline data acquired in 2017 and the monitor in 2023. Tillostson et al. (2019) demonstrated the value of the dense acquisition on 3D static images. Romanenko et al. (2023) applied 3D DM FWI to the baseline data and successfully reconstructed high-resolution baseline model, which laid the groundwork for this 4DFWI application.

For this pilot test of 4DFWI, some 480 common receiver gathers along 5 OBN lines are selected from both baseline and monitor datasets for the test. Receiver nodes within 25m from each other and shots within 15m are selected from both. After receivers and shots selection, the baseline and monitor datasets have closely matching source-receiver geometries.

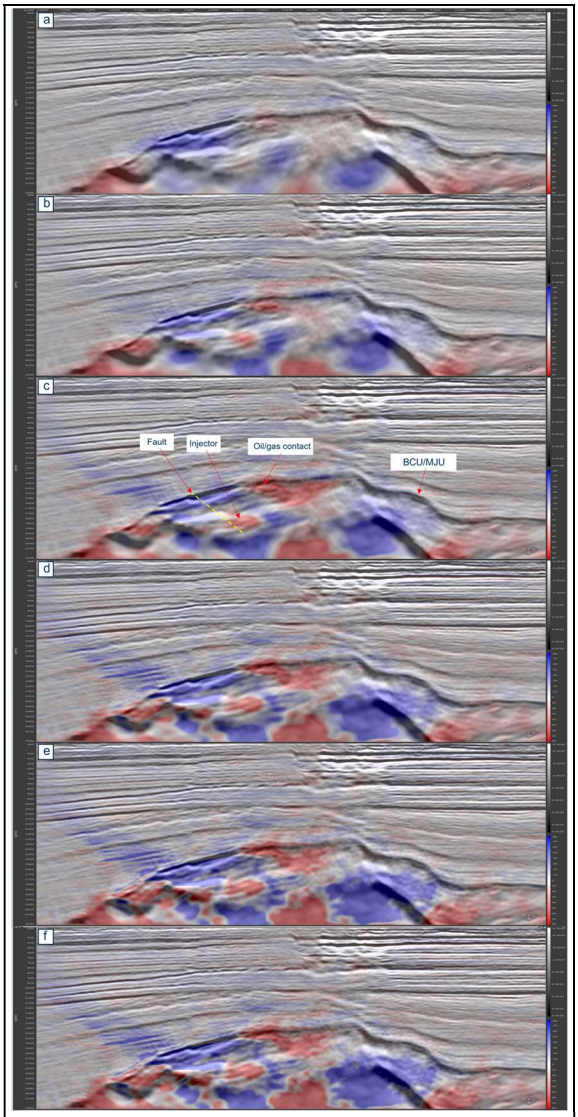

Figure 1: 4D model from 5Hz(a), 10Hz(b), 20Hz(c), 30Hz(d), 40Hz(e) and 50Hz(f) joint inversion, all overlaid with an RTM image using the initial model. The main reflector, base of Cretaceous Unconformity (BCU), and interpretations of 4D model are indicated in (c) only.

Key learnings from the legacy 3DFWI study of Romanenko et al. (2023) have been applied in this 4DFWI test. The OBN data provides reliable low frequency down to around 2Hz. The low-cut part of the bands inverted in this study is kept at

DOI:10.1190/4D-Forum2024-015.1

1.5-2Hz. It has been also determined through analysis that little diving waves energy was returning from the reservoir level which is beneath the base of Cretaceous unconformity (BCU) and the updates in the reservoir section primarily rely on reflection data. Therefore reflection data that have been gone through basic pre-processing steps are mainly inverted in this 4DFWI test.

Both datasets have been inverted by joint inversion in six bands sequentially up to 50-60Hz. The initial model is originated from a legacy smooth model derived by using the baseline data through a workflow involving reflection tomography and FWI using diving waves. Since BCU is a strong reflector and the reservoir section was not well sampled by diving waves, the initial background model in the overburden is more accurate than in the reservoir section below. With that considered, the overburden and the reservoir section below have been updated in the joint inversion using gradients derived differently, with that for the reservoir emphasizing the lower wavenumber updating than that for the overburden.

Figure 1 shows the updated 4D models from sequentially inverting six bands in joint inversion with high-cut at 5-8Hz, 10-20Hz, 20-30Hz, 30-40Hz, 40-50Hz and 50-60Hz, respectively. In the alternative model updates, either model is updated for n=2 iterations before the next alternation to update the other model. The damping coefficient is determined for each band such that the third term of model regularization in Equation (2) is numerically around 10% of the other two terms, meaning that in the reflection 4DFWI joint inversion, the damping coefficient decreases with the higher frequency being inverted since more details in the model usually increase the model differences. The norm of the 4D model difference for this test was p=2.

The 4D model displayed in Figure 1 shows that the resolution is improved with increasing frequency band being inverted. Most updates concentrate in the reservoir below the BCU and the minor updates in the overburden conforms to the geological structures well. The revealed 4D anomalies in the reservoir have been identified as the oil/gas contact and the injector which tends to harden the area surrounding it, which is confirmed by the positive 4D anomaly. Compared to the 40Hz 4D model in Figure 1(e), the resolution improvement in the 4D model from 50Hz joint inversion (Figure 1(f)) is minimum, consistent with the observation that the signals sampling the reservoir are minimum beyond 50Hz. The absolute amplitudes in the 50Hz 4D model could reach up to about 2.5% of the background model. The edge anomaly seen on the left part of the 4D model is most probably related to the edge effects from limited acquisition coupled with the model structures there.

Discussions and conclusions

This study proposes a 4D joint inversion in the framework of DM FWI. It updates the baseline and monitor models in a coordinated way since the two models interact with each other during the optimization process of waveform inversion. The algorithm does not require both the baseline and monitor datasets to have an identical source-receiver geometry, which enables a shorter turn-around by avoiding data regularization to align the two datasets.

The application of the 4D joint inversion to two datasets acquired roughly six years apart over a production field in the North Sea recovers 4D signals matching expected anomalies localized at the reservoir level. These include the oil/gas contact, hardening observed at the well injector and the softening of the producing fields indicated by the negative 4D velocity anomalies. Future work will concentrate on further 4D model validation and potentially elastic 4D FWI.

Acknowledgements

We wish to thank the Clair Joint Venture group (BP, Shell, Chevron & Harbour) for permission to present the field data, and TGS for permission to publish this work. We also want to thank Bin Wang for helpful discussions and Darren Kozlek and Matt Yates for HPC support.

REFERENCES

Anderson, R., A. Boulanger, W. He, L. Xu, P. B. Flemings, T. D. Burkhart and A. R. Hoover, 2005. 4D time-lapse seismic monitoring in the South Timbalier 295 field, Gulf of Mexico. SEG Annual Meeting, 2005.

Dutta, G., E. Saragoussi, X. Cheng, Y. Zhai, C. Parekh and D. Vigh, 2023. EAFE Annual Meeting, 2023.

Gao, F., S. Dong, Y. He, J. Shen, F. Liu, B. Wang and C. Calderon, Y. Ivanov, F. Marcy and O. E. Aaker, 2023. High resolution image by dynamic matching FWI in the presence of AVO effects, SEG Annual Meeting, 2023.

Liu, Y. and I. Tsvankin, 2022. Source-independent time-lapse full-waveform inversion for anisotropic media. Geophysics, 2022, Vo. 87, NO. 1, P. R111-122.

Lumley, D. E., 2021. Time-lapse seismic reservoir monitoring. Geophysics, V. 66, Issue 1, 2001.

Romanenco, M., L. Saxton, D. Davies, F. Liu, J. Gromotka, Y. He, 2023. High-frequency FWI on Clair OBN dataset – challenges and successes. IMAGE, 2023.

DOI:10.1190/4D-Forum2024-015.1

Meek, R., K. Woller, M. George, R. Hullm H. Bello and J. Wagner, 2017. Time-lapse imaging of a hydraulic stimulation using 4D Vertical Seismic profiles and fiber optics in the Midland Basin.

Mao, J., J. Sheng, Y. Huang, F. Hao and F. Liu, 2020, Multi-Channel dynamic matching full-waveform inversion, SEG Technical Program Expanded Abstracts.

Musa, M. B. Biondi and M. Meadows, 2015. Simultaneous TV-regularized time-lapse FWI with application to field data. SEG Annual Meeting, 2015.

Pintus, A., H. Ayadi and N. Salaun, 2023. Time-lapse FWI to improve understanding of superimposed reservoirs in deep offshore. EAGE Annual Meeting, 2023.

Routh, P., S. Nayak, J. Dorsett, K. Banerji, Y. H. Cha, V. Gottumukkula, G. Palacharla and V. Gudipati, 2023. Value of elastic full-wavefiel inversion in derisking clastic reservoirs in presence of noise. SEG Annual Meeting, 2023.

Sirgue, L, B. Denel and F. Gao, 2011. Integrating 3D full waveform inversion into depth imaging projects, 2011. SEG International Exposition 2011 Annual Meeting.

Tillotson, P., D. Davies, M. Ball, and L. Smith [2019]. Clair Ridge: Learnings From Processing the Densest OBN Survey in the UKCS: 81st EAGE Conference and Exhibition 2019, Jun 2019, Volume 2019, p.1 - 5

Yang, D., M. Fehler, A. Malcolm, F. Liu and S. Morton, 2013. Double difference waveform inversion of 4D ocean bottom cable data: application to Valhall, North Sea, SEG Annual Meeting, 2013.

Yong, S.L., M Cvetkovic, T. Johnson, B. Soelistijo and L. Ge, 2023. Resolving geological complexity with legacy streamer survey: Potiguar 3D offshore Brazil case study. IMAGE, 2023.

Zhou, W. and D. Lumley, 2020. Non-repeatability on time-lapse 4D seismic full waveform inversion. SEG Annual Meeting, 2020.

